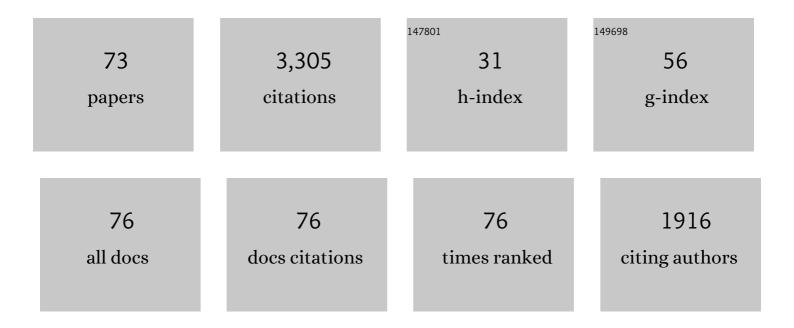
List of Publications by Year in descending order

Source: https://exaly.com/author-pdf/3987199/publications.pdf Version: 2024-02-01



#	Article	IF	CITATIONS
1	Evaluation of short-term temporal evolution of Pluto's surface composition from 2014–2017 with APO/TripleSpec. Icarus, 2022, 373, 114729.	2.5	4
2	Orbits and Occultation Opportunities of 15 TNOs Observed by New Horizons. Planetary Science Journal, 2022, 3, 23.	3.6	3
3	Anomalous Flux in the Cosmic Optical Background Detected with New Horizons Observations. Astrophysical Journal Letters, 2022, 927, L8.	8.3	32
4	The Diverse Shapes of Dwarf Planet and Large KBO Phase Curves Observed from New Horizons. Planetary Science Journal, 2022, 3, 95.	3.6	10
5	A Near-surface Temperature Model of Arrokoth. Planetary Science Journal, 2022, 3, 110.	3.6	9
6	The Geophysical Environment of (486958) Arrokoth—A Small Kuiper Belt Object Explored by <i>New Horizons</i> . Journal of Geophysical Research E: Planets, 2022, 127, .	3.6	18
7	Origins of pits and troughs and degradation on a small primitive planetesimal in the Kuiper Belt: high-resolution topography of (486958) Arrokoth (aka 2014 MU69) from New Horizons. Icarus, 2021, 356, 113834.	2.5	5
8	Photometry of Kuiper belt object (486958) Arrokoth from New Horizons LORRI. Icarus, 2021, 356, 113723.	2.5	13
9	A statistical review of light curves and the prevalence of contact binaries in the Kuiper Belt. Icarus, 2021, 356, 114098.	2.5	10
10	Persephone: A Pluto-system Orbiter and Kuiper Belt Explorer. Planetary Science Journal, 2021, 2, 75.	3.6	7
11	Pluto's Sputnik Planitia: Composition of geological units from infrared spectroscopy. Icarus, 2021, 359, 114303.	2.5	5
12	On Charon's Far-ultraviolet Surface Reflectance. Planetary Science Journal, 2021, 2, 164.	3.6	0
13	Size and Shape of (11351) Leucus from Five Occultations. Planetary Science Journal, 2021, 2, 202.	3.6	7
14	New or Increased Cometary Activity in (2060) 95P/Chiron. Research Notes of the AAS, 2021, 5, 211.	0.7	3
15	New Horizons Observations of the Cosmic Optical Background. Astrophysical Journal, 2021, 906, 77.	4.5	42
16	Spitzer's Solar System studies of asteroids, planets and the zodiacal cloud. Nature Astronomy, 2020, 4, 940-946.	10.1	7
17	Size and Shape Constraints of (486958) Arrokoth from Stellar Occultations. Astronomical Journal, 2020, 159, 130.	4.7	25
18	The Complex Rotational Light Curve of (385446) Manwë–Thorondor, a Multicomponent Eclipsing System in the Kuiper Belt. Astronomical Journal, 2020, 159, 27.	4.7	1

#	Article	IF	CITATIONS
19	Color, composition, and thermal environment of Kuiper Belt object (486958) Arrokoth. Science, 2020, 367, .	12.6	64
20	The geology and geophysics of Kuiper Belt object (486958) Arrokoth. Science, 2020, 367, .	12.6	76
21	The solar nebula origin of (486958) Arrokoth, a primordial contact binary in the Kuiper Belt. Science, 2020, 367, .	12.6	79
22	Disk-resolved Photometric Properties of Pluto and the Coloring Materials across its Surface. Astronomical Journal, 2020, 159, 74.	4.7	18
23	Photometric Analyses of Saturn's Small Moons: Aegaeon, Methone, and Pallene Are Dark; Helene and Calypso Are Bright. Astronomical Journal, 2020, 159, 129.	4.7	8
24	Influence of Solar Disturbances on Galactic Cosmic Rays in the Solar Wind, Heliosheath, and Local Interstellar Medium: Advanced Composition Explorer, New Horizons, and Voyager Observations. Astrophysical Journal, 2020, 905, 69.	4.5	15
25	Phase Curves from the Kuiper Belt: Photometric Properties of Distant Kuiper Belt Objects Observed by New Horizons. Astronomical Journal, 2019, 158, 123.	4.7	14
26	The HST lightcurve of (486958) 2014 MU69. Icarus, 2019, 334, 11-21.	2.5	13
27	Detection of ammonia on Pluto's surface in a region of geologically recent tectonism. Science Advances, 2019, 5, eaav5731.	10.3	49
28	Initial results from the New Horizons exploration of 2014 MU ₆₉ , a small Kuiper Belt object. Science, 2019, 364, .	12.6	113
29	New Horizons Photometry of Pluto's Moon Charon. Astrophysical Journal Letters, 2019, 874, L3.	8.3	8
30	The distribution of H2O, CH3OH, and hydrocarbon-ices on Pluto: Analysis of New Horizons spectral images. Icarus, 2019, 331, 148-169.	2.5	21
31	The color and binarity of (486958) 2014 MU69 and other long-range New Horizons Kuiper Belt targets. Icarus, 2019, 334, 22-29.	2.5	12
32	Phase Curves of Nix and Hydra from the New Horizons Imaging Cameras. Astrophysical Journal Letters, 2018, 852, L35.	8.3	6
33	The New Horizons and Hubble Space Telescope search for rings, dust, and debris in the Pluto-Charon system. Icarus, 2018, 301, 155-172.	2.5	11
34	lces on Charon: Distribution of H2O and NH3 from New Horizons LEISA observations. Icarus, 2018, 300, 21-32.	2.5	38
35	Limits on Dione's Activity Using Cassini/CIRS Data. Geophysical Research Letters, 2018, 45, 5876-5898.	4.0	2
36	Composition of Pluto's small satellites: Analysis of New Horizons spectral images. Icarus, 2018, 315, 30-45.	2.5	49

#	Article	IF	CITATIONS
37	Great Expectations: Plans and Predictions for New Horizons Encounter With Kuiper Belt Object 2014 MU ₆₉ ("Ultima Thuleâ€). Geophysical Research Letters, 2018, 45, 8111-8120.	4.0	14
38	High-precision Orbit Fitting and Uncertainty Analysis of (486958) 2014 MU69. Astronomical Journal, 2018, 156, 20.	4.7	39
39	Inflight radiometric calibration of New Horizons' Multispectral Visible Imaging Camera (MVIC). Icarus, 2017, 287, 140-151.	2.5	14
40	Physical state and distribution of materials at the surface of Pluto from New Horizons LEISA imaging spectrometer. Icarus, 2017, 287, 229-260.	2.5	99
41	Pluto's global surface composition through pixel-by-pixel Hapke modeling of New Horizons Ralph/LEISA data. Icarus, 2017, 287, 218-228.	2.5	95
42	Global albedos of Pluto and Charon from LORRI New Horizons observations. Icarus, 2017, 287, 207-217.	2.5	82
43	Charon's light curves, as observed by New Horizons' Ralph color camera (MVIC) on approach to the Pluto system. Icarus, 2017, 287, 152-160.	2.5	2
44	THE FIRST HIGH-PHASE OBSERVATIONS OF A KBO: NEW HORIZONS IMAGING OF (15810) 1994 JR ₁ FROM THE KUIPER BELT. Astrophysical Journal Letters, 2016, 828, L15.	8.3	14
45	Reorientation of Sputnik Planitia implies a subsurface ocean on Pluto. Nature, 2016, 540, 94-96.	27.8	108
46	The formation of Charon's red poles from seasonally cold-trapped volatiles. Nature, 2016, 539, 65-68.	27.8	44
47	The atmosphere of Pluto as observed by New Horizons. Science, 2016, 351, aad8866.	12.6	201
48	The small satellites of Pluto as observed by New Horizons. Science, 2016, 351, aae0030.	12.6	78
49	The geology of Pluto and Charon through the eyes of New Horizons. Science, 2016, 351, 1284-1293.	12.6	219
50	Surface compositions across Pluto and Charon. Science, 2016, 351, aad9189.	12.6	242
51	Small particles dominate Saturn's Phoebe ring to surprisingly large distances. Nature, 2015, 522, 185-187.	27.8	16
52	The Pluto system: Initial results from its exploration by New Horizons. Science, 2015, 350, aad1815.	12.6	407
53	Thermophysical property variations across Dione and Rhea. Icarus, 2014, 241, 239-247.	2.5	23
54	The UT 7/8 February 2013 Sila–Nunam mutual event & future predictions. Icarus, 2014, 229, 423-427.	2.5	6

#	Article	IF	CITATIONS
55	The rotational light curve of (79360) Sila–Nunam, an eclipsing binary in the Kuiper Belt. Icarus, 2014, 236, 72-82.	2.5	5
56	Photometric Properties of Solar System Ices. Astrophysics and Space Science Library, 2013, , 47-72.	2.7	5
57	Mutual events in the Cold Classical transneptunian binary system Sila and Nunam. Icarus, 2012, 220, 74-83.	2.5	28
58	A high-amplitude thermal inertia anomaly of probable magnetospheric origin on Saturn's moon Mimas. Icarus, 2011, 216, 221-226.	2.5	57
59	Comparing Phoebe's 2005 opposition surge in four visible light filters. Icarus, 2011, 212, 819-834.	2.5	11
60	Photometry of Triton 1992–2004: Surface volatile transport and discovery of a remarkable opposition surge. Icarus, 2011, 212, 835-846.	2.5	33
61	Saturn's largest ring. Nature, 2009, 461, 1098-1100.	27.8	134
62	Enceladus: Cosmic Graffiti Artist Caught in the Act. Science, 2007, 315, 815-815.	12.6	98
63	The opposition surge of Enceladus: HST observations 338–1022 nm. Icarus, 2005, 173, 66-83.	2.5	59
64	Reflectance Spectroscopy of Icy Surfaces. Astrophysics and Space Science Library, 1998, , 157-197.	2.7	26
65	Re-Analysis of the Solar Phase Curves of the Icy Galilean Satellites. Icarus, 1997, 128, 49-74.	2.5	85
66	The Scattering Properties of Natural Terrestrial Snows versus Icy Satellite Surfaces. Icarus, 1997, 128, 28-48.	2.5	34
67	A Photometric Study of Enceladus. Icarus, 1994, 110, 155-164.	2.5	25
68	Mimas: Photometric roughness and albedo map. Icarus, 1992, 99, 63-69.	2.5	33
69	Backscattering from frost on icy satellites in the outer Solar System. Nature, 1990, 347, 162-164.	27.8	38
70	Scattering properties of natural snow and frost: Comparison with icy satellite photometry. Icarus, 1990, 88, 418-428.	2.5	39
71	Voyager Disk-Integrated Photometry of Triton. Science, 1990, 250, 419-421.	12.6	41
72	Albedo dichotomy of Rhea: Hapke analysis of Voyager photometry. Icarus, 1989, 82, 336-353.	2.5	47

#	Article	IF	CITATIONS
73	Estimating phase integrals: A generalization of Russell's law. Icarus, 1988, 73, 324-329.	2.5	6